System Identification using CFD Captive and Free Running Tests in Severe Stern Waves

Motoki Araki[1], Hamid Sadat-Hosseini[2], Yugo Sanada[2], Naoya Umeda[3], and Frederick Stern[2]

[1] National Maritime Research Institute, Japan

[2] IIHR - Hydroscience & Engineering, The University of Iowa, USA

[3] Department of Naval Architecture and Ocean Engineering, Osaka University, Japan

ABSTRACT

Predicting ship maneuverability and stability in stern waves are important topics to prevent dangeraous roll-manuevering motion such as broaching. The convensional mathematical maneuvering and wave models have some difficulities predicting ship motions in waves while CFD free running simulations show quantitative agreement with the experiments. Therefore a few CFD free running and captive simulation results are applied to tune the mathematical maneuvering and wave model by using system identification techniques. For simulating free running in moderate waves, the tuned model shows better agreement with the experiments than the original simulation model. Though, in more severe wave condition, the tuned model shows some difficulty to predict violent motions specifically in broaching.

KEYWORDS

System identification; Maneuvering; Seakeeping; Wave model

INTRODUCTION

Nowadays, intact ships need to have reasonable stability and maneuverability in waves. Especially, they are required to avoid broaching in quartering and stern waves, which is recognized as one of the major stability failure modes (IMO, 2012) in the 54th session of International Maritime Organization (IMO) Sub-committee on Stability and Load Lines and Fishing Vessels Safety (SLF)..

To assess the ship stability and maneuverability in waves and prevent the broaching, reasonable numerical simulation method needs to be elected. It is true that experimental fluid dynamic (EFD) using ship model and wave basin is one of the most reliable methods but it is too expensive and time consuming to exam all suspicious conditions.

One of the strong candidates is system-based (SB) method. The SB approach in this paper means an approach consisting of two layered sub systems. In the lower layer, hydrodynamic forces mainly due to potential flow are calculated by solving partial differential equations of potential flow and hydrodynamic forces mainly due to viscosity flow are estimated with captive model experiments or empirical formulas. In the upper layer, ship motions are calculated by solving ordinary differential equations with initial conditions. Some of the researches using this approach provide qualitative agreement with experimental free running for fishing vessels in broaching prediction (Umeda, 1999). To assess the risk of broaching, huge number of simulations is needed to sweep out the suspicious wave and operational conditions. However it is also true that the SB method shows some difficulty for quantitative agreement with experimental free running results for a unconventional ship, ONR tumblehome vessel (Araki et al., 2010). For generic usage, the simulation method needs to be available for any type of ships. Moreover, for reasonable SB simulations, large number of captive model tests is necessary to estimate maneuvering coefficients.

Meanwhile, with remarkable developments of computer technologies, computational fluid dynamics (CFD) become practical tool for naval architects. Moreover, several CFD simulations showed quantitative agreement with experimental free running results even in sever waves (Sadat-Hosseini et al., 2011). Therefore, CFD simulation has potential to replace the model experiments. The CFD simulation not only cuts the cost of experiments but provides fruitful information including the hydrodynamic force acting on the ship and the flow field around her, while EFD free running simulation merely provides ship motions. However, large computational time is required for CFD free running simulation even with recent supercomputers. Therefore, CFD simulations for all dangerous conditions are not realistic in this period.

Considering the pros and cons of SB and CFD methods, the authors proposed SB free running simulation using system identification with CFD free running results. A few CFD free running simulation results are used to predict maneuvering coefficients for SB model by appling system identification techniques. For the first step for broaching prediction, the proposed method is applied for calm water cases and it successfully predicts ship maneuvering (Araki et al., 2012a). Then, Araki et al. (2012b) extended this methodology to the case in moderate astern waves with a reference wave force model. In this paper, the reference wave model is first revised and then applied to more severe wave cases such as broaching.

SUBJECT SHIP

The 1/49 scaled model of ONR tumblehome (ONRTH), which was developed at Naval Surface Warfare Center (Bishop et al., 2005), appended with skeg, bilge keels, rudders, shafts with propeller shaft brackets and twin propellers was used for the free running experiments. The main particulars of the ONRTH ship are listed in Table 1. The details of the body plan is shown in Fig. 1.

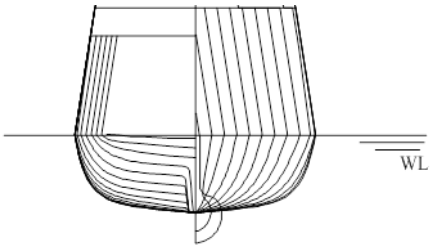

Fig.1 Body plan of the ONRTH model.

Table 1 Principal particulars of the ONRTH

	Model scale
Length: L	3.147 m
Breadth: B	0.384 m
Depth: D	0.266 m
Draft: d	0.112 m
Displacement: W	72.6 kg
Metacentric height: GM	0.0424 m
Natural roll period: T_ϕ	1.644 s
Rudder area: A_R	0.012 m^2 × 2
Block coefficient: C_b	0.535
Vertical position of CoG from waterline (downward positive): OG	-0.392 × d
Radius of gyration in pitch: κ_{yy}	0.25 × L
Maximum rudder angle: δ_{max}	± 35°

CFD METHOD

The code CFDShip-Iowa v4 (Carrica et al., 2010) is used for the CFD computations. The CFDShip-Iowa is an overset, block structured CFD solver designed for ship applications using either absolute or relative inertial non-orthogonal curvilinear coordinate system for arbitrary moving but non-deforming control volumes. Turbulence models include blended k-ε/k-ω based isotropic and anisotropic Raynolds Averaged Navier Stokes (RANS), and (detached eddy simulations) DES approaches with near-wall or wall functions. A simplified body force model is used for the propeller, which prescribes axisymmetric body force with axial and tangential components.

The propeller model requires the open water curves and advance coefficients as input and provides the torque and thrust forces. The open water curves are defined as a second order

polynomial fit of the experimental $K_T(J)$ and $K_Q(J)$ curves. The advance coefficient is computed using ship speed with neglecting the wake effects. Herein, two PID controllers are used. The heading controller acting on the rudders are responsible to turn the rudders to keep the ship in the desired direction. The speed controller acting on the body force propeller model is responsible to rotate the propellers at appropriate propeller rate to keep the ship at the desired speed. The heading controller uses P=1 for the proportional gain and zero for both the integral and derivative gains mimicking EFD setup.

Table 2 Grids for free model simulations.

Name	**Size (grid points)**	**# of procs**	**Type**
Hull S/P*	199x61x104 (1.26 M x2)	12 (x2)	Double O
Skeg S/P	61x49x40 (0.12 M x2)	1 (x2)	O
Bilge Keel S/P	99x45x50 (0.23 M x2)	2 (x2)	H
Rudder Root Collar S/P	121x35x28 (0.12 M x2)	1 (x2)	O
Rudder Root Gap S/P	121x51x19 (0.12 M x2)	2 (x2)	Conformal to Collar
Rudder Outer S/P	61x36x55 (0.12 M x2)	1 (x2)	Double O
Rudder Inner S/P	61x36x55 (0.12 M x2)	1 (x2)	Double O
Rudder Gap S/P	121x51x19 (0.12 M x2)	2 (x2)	Conformal to Inner and Outer
Shaft Collar S/P	39x50x57 (0.11 M x2)	1 (x2)	O
Shaft Proper S/P	74x41x37 (0.11 M x2)	1 (x2)	O
Shaft Tip S/P	110x117x100 (1.29 M x2)	12 (x2)	O with end pole
Strut Outer S/P	69x34x50 (0.12 M x2)	1 (x2)	O
Strut Inner S/P	69x34x50 (0.12 M x2)	1 (x2)	O
Superstructure	165x61x85 (0.86 M)	8	Wrap
Refinement	145x81x113 (1.33 M)	12	Cartesian
Background	213x84x113 (2.02 M)	20	O
Total	**(12.1 M)**	**116**	

* S/P: Starboard/Port

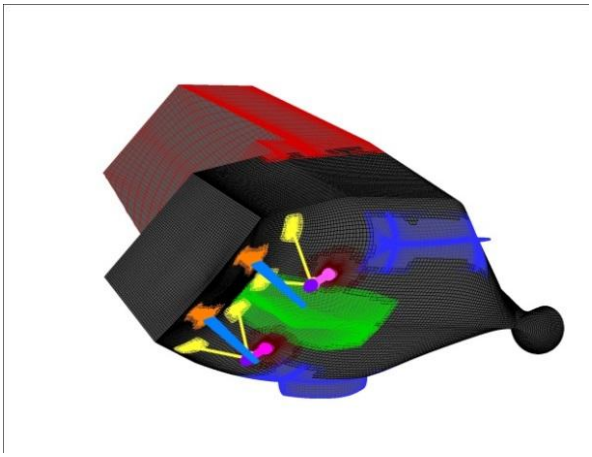

Fig.2 CFD overset grids for ONRTH hull and appendages.

The CFD initial condition is different with EFD in several ways. The CFD model was accelerated with infinite rate to the target speed unlike EFD. Then the model was towed at target speed which was constant while the model was only free to heave and pitch and not roll until the wave trough was located at midship. After that, the model was released and rudder controller was activated immediately to start maneuvering. The differences between EFD and CFD setup might cause some discrepancies between EFD and CFD results.

The model is appended with skeg, bilge keels, superstructure, rudders, rudder roots, shafts, and propeller brackets same as the EFD model but not appended with actual propellers. The computational grids are overset with independent grids for the hull, superstructure, appendages, refinement and background, and then assembled together to generate the total grid. The total number of grid points is 12.1 M for free model simulations. Details of the grids are shown in Table 2 and Fig. 2. The free running in waves and calm water verification studies are performed by Sadat-Hosseini et al. (2011) and Araki et al. (2012a), which showed quantitative agreement with EFD results.

EFD METHOD

To validate the CFD and SB simulation, EFD free running were executed in Iowa institute of hydraulic research, USA (IIHR) wave basin facility and National Research Institute of Fisheries Engineering, Japan (NRIFE) seakeeping and maneuvering basin (Fig.3). The EFD data in calm water and moderate waves were provided from the IIHR basin and severe wave cases were from the NRIFE basin.

The IIHR wave basin has dimensions of 40×20 square meters with 3 meters water depth and is designed to test captive or radio-controlled model scale ships. There are six plunger-type wave makers on the one side of the basin to generate regular or irregular waves. The x-direction (length) main-carriage and y-direction (width) sub-carriage with yaw-direction turntable (heading) are installed tracking and launching the model. The plane trajectories of the ship maneuvering were captured by tracking cameras chasing two LED lights placed on the deck of a model. The ship motion, roll, pitch and yaw rates/angle were recorded by an onboard fiber optical gyroscope (FOG). The initial condition of free running can be controlled by the auto-launch system. A more detail description of the IIHR wave basin is provided by Sanada et al. (2012).

The NRIFE basin has dimensions of 60×25 square meters with 3.2 meters water depth and is designed to test captive or radio-controlled model scale ships. There are 80 plunger-type wave makers on the one side of the basin to generate regular or irregular waves. The x-direction (length) main-carriage and y-direction (width) sub-carriage with yaw-direction turntable (heading) are installed to tow a model. The trajectories are measured by a total station automatically chasing a prisms setting on a model ship (Furukawa et al., 2012). The ship rotation motions were measured with FOG. Moreover the rudder normal force was measured with strain gages pasted on the rudder shafts. Not like IIHR basin, the model was released manually in NRIFE. Therefore it was difficult to control initial condition during the free running in waves.

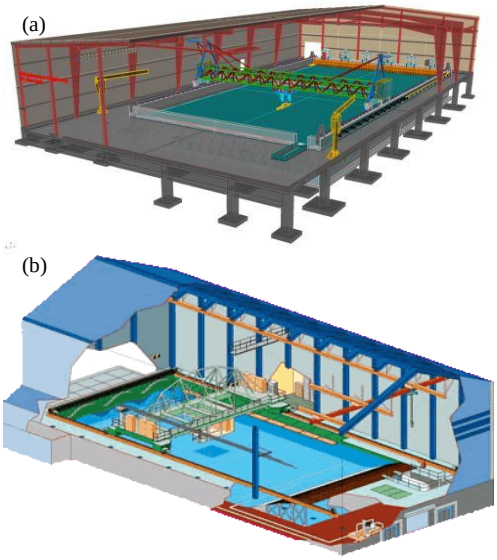

Fig.3 Drawing of (a) IIHR wave basin; (b) NRIFE seakeeping and maneuvering basin.

SB METHOD

(1) Maneuvering Mathematical Model

One of the most reliable maneuvering models is the maneuvering mathematical modeling group (MMG) model (Ogawa and Kasai, 1978; Ogawa et al., 1980). To simulate the maneuvering and roll motions in stern waves, coupled 4DOF (surge-sway-roll-yaw) model based on the MMG model is used in this paper as shown in Eqs. (1)-(4). Similar 4DOF models were already applied to predict broaching and have some certain results (Umeda et al., 2008; Hashimoto et al., 2011). Horizontal body axes, shown in Fig.4, are used for the coordinate system (Hamamoto and Kim, 1993). MMG rudder model (Ogawa et al., 1980) is used for rudder forces/moments. Here the maneuvering and rudder coefficients are tuned by the system identification in calm water maneuvers (Araki et al., 2012a). A constrained least square (CLS) method using generalized reduced gradient algorithm (Lasdon et al., 1978) is used for the system identification. The corrected coefficients are compared with the original coefficients estimated by towing tests or empirical formulas in Table 3. The maneuvering simulation in calm water using these tuned coefficients gives much

better agreement with EFD than using original coefficients, as shown in Fig.5.

$$(m+m_x)\dot{u}-(m+m_y)vr=T(u;n)-R(u)+X_{vr}(u)vr +X_{rr}(u)r^2+X_{vv}(u)v^2+X_R(\delta,u,v,r) \quad (1)$$

$$(m+m_y)\dot{v}+(m+m_x)ur=Y_v(u)v+Y_r(u)r+Y_\phi(u)\phi +Y_{vvv}(u)v^3+Y_{vvr}(u)v^2r+Y_{vrr}(u)r^2v+Y_{rrr}(u)r^3+Y_R(\delta,\phi,u,v,r) \quad (2)$$

$$(I_x+J_x)\dot{p}=m_x z_H ur+K_v(u)v+K_r(u)r+K_p(u)p +K_\phi(u)\phi-mgGZ(\phi)+K_{vvv}(u)v^3+K_{vvr}(u)v^2r +K_{vrr}(u)r^2v+K_{rrr}(u)r^3+K_R(\delta,u,v,r) \quad (3)$$

$$(I_z+J_z)\dot{r}=N_v(u)v+N_r(u)r+N_\phi(u)\phi+N_{vvv}(u)v^3 +N_{vvr}(u)v^2r+N_{vrr}(u)r^2v+N_{rrr}(u)r^3+N_R(\delta,\phi,u,v,r) \quad (4)$$

Table 3 Values of original and SI-calm maneuvering and rudder coefficients used in 4-DOF nonlinear SB model.

Coef.	Orig.	SI-calm	**Coef.**	Orig.	SI-calm
ε	1.0	0.75	Y_{vrr}	-0.80	0.32
γ_R	0.70	0.55	Y_{rrr}	0.174	0.080
l_R/L	-1.00	-0.95	Y_ϕ	-5.1e-04	-6.5E-04
t_R	0.30	0.10	J_{xx}	4.1e-05	1.0e-4
a_H	0.25	0.23	z_H	0.852	1.08
z_{HR}/d	0.854	0.802	K_p	-0.243	-0.203
x_H/L	-0.45	-0.52	K_ϕ	6.3e-04	9.8E-04
m_x	0.0131	0.0	J_{zz}	0.0079	0.0059
X_{vv}	-0.0858	-0.070	N_v	-0.0932	-0.0851
X_{vr}	0.0522	0.065	N_r	-0.0549	-0.0395
X_{rr}	-0.0213	-0.025	N_{vvv}	-0.532	-0.492
m_y	0.109	-0.070	N_{vvr}	-0.629	-0.805
Y_v	-0.30	-0.20	N_{vrr}	-0.139	-0.121
Y_r	-0.0832	0.07	N_{rrr}	-4.46e-3	-6.50e-3
Y_{vvv}	-1.77	-2.0	N_ϕ	-5.11e-3	-9.89e-3
Y_{vvr}	0.262	0.32			

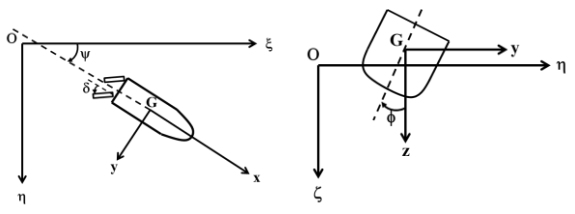

Fig.4 Coordinate system for 4DOF SB model.

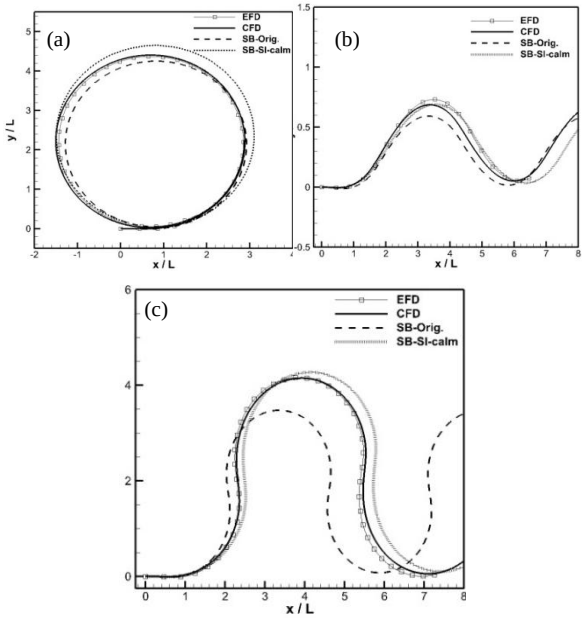

Fig.5 Trajectories of EFD, CFD, SB-Orig., and SB-SI free running in calm water: (a) δ=25deg turning circle; (b) ψ/ δ=20/20 zigzag; (c) ψ/ δ=90/35 large angle zigzag.

(1) Wave Force/Effect Model

In stern waves, the dominant wave forces are Froude-Krylov (FK) and diffraction forces. However, on the ONRTH, the simple FK and diffraction forces model cannot predict actual wave force quantitatively (Hashimoto et al., 2011). Therefore, several tuning parameters and several wave effects are taken into account for the wave model. It is known that wave particle velocity affects the rudder inflow velocity (e.g. Hashimoto et al., 2004). Moreover, Son and Nomoto (1982) showed the maneuvering coefficients variations due to wave are one of the important factors for course keeping stability in wave, which is critical for broaching prediction. Therefore FK, diffraction forces, wave particle velocity on rudder force, and the maneuvering coefficients variations are taken into account as showed in Eqs. (5)-(11). The wave-induced forces are optimized by fixing the FK forces and tuning the diffraction forces. The parameters (a_1, b_1, c_1, d_1, ε_{a1}, ε_{b1}, ε_{c1}, ε_{d1}) tune the amplitudes and phases of the diffraction forces. For the surge wave force, , the tuning parameters are set on the FK force due to the difficulty of computing the surge diffraction force with the slender body theory. The tuning

parameters β_1 and β_2 are for the wave particle velocities on rudder normal force and parameters $a_{2,3,4}$, $b_{2,3}$, $c_{2,3}$, $d_{2,3}$, $\varepsilon_{a2,3,4}$, $\varepsilon_{b2,3}$, $\varepsilon_{c2,3}$ and $\varepsilon_{d2,3}$ are for the maneuvering coefficients variations. It should be noted that the maneuvering coefficients variations are applied for the major maneuvering coefficients (X_{vv}, X_{vr}, X_{rr}, Y_v, Y_r, K_v, K_r, N_v, N_r). All initial tuning parameters are zero except the parameters for diffraction amplitudes, which are 1.0.

$$\begin{aligned} X_W &= \hat{X}_W^{FK}(a_1,\varepsilon_{a1}) + k\zeta_w\left(a_2\sin(k\xi_G+\varepsilon_{a2})\cdot X_{vv}\cdot v^2\right. \\ &\left. +a_3\sin(k\xi_G+\varepsilon_{a3})\cdot X_{vr}\cdot vr + a_4\sin(k\xi_G+\varepsilon_{a4})\cdot X_{rr}\cdot r^2\right) \end{aligned} \quad (5)$$

$$\begin{aligned} Y_W &= Y_W^{FK} + \hat{Y}_W^{Dif}(b_1,\varepsilon_{b1}) \\ &+k\zeta_w\left(b_2\sin(k\xi_G+\varepsilon_{b2})\cdot Y_v\cdot v + b_3\sin(k\xi_G+\varepsilon_{b3})\cdot Y_r\cdot r\right) \end{aligned} \quad (6)$$

$$\begin{aligned} K_W &= K_W^{FK} + \hat{K}_W^{Dif}(c_1,\varepsilon_{c1}) \\ &+k\zeta_w\left(c_2\sin(k\xi_G+\varepsilon_{c2})\cdot K_v\cdot v + c_3\sin(k\xi_G+\varepsilon_{c3})\cdot K_r\cdot r\right) \\ &+OG\cdot Y_W \end{aligned} \quad (7)$$

$$\begin{aligned} N_W &= N_W^{FK} + \hat{N}_W^{Dif}(d_1,\varepsilon_{d1}) \\ &+k\zeta_w\left(d_2\sin(k\xi_G+\varepsilon_{d2})\cdot N_v\cdot v + d_3\sin(k\xi_G+\varepsilon_{d3})\cdot N_r\cdot r\right) \end{aligned} \quad (8)$$

$$F_N = \frac{1}{2}\rho A_R\left(\hat{u}_{Rw}{}^2+\hat{v}_{Rw}{}^2\right) f_\alpha\cdot\sin\hat{\alpha}_R \quad (9)$$

$$\begin{cases} \hat{X}_W^{FK} = a_1 A_X \sin\left(k\xi_G+\varepsilon_X+\varepsilon_{a1}\right) \\ \hat{Y}_W^{Dif} = b_1 A_Y \sin\left(k\xi_G+\varepsilon_Y+\varepsilon_{b1}\right) \\ \hat{K}_W^{Dif} = c_1 A_K \sin\left(k\xi_G+\varepsilon_K+\varepsilon_{c1}\right) \\ \hat{N}_W^{Dif} = d_1 A_N \sin\left(k\xi_G+\varepsilon_N+\varepsilon_{d1}\right) \end{cases} \quad (10)$$

$$\begin{cases} \hat{u}_{Rw} = u_R + \beta_1\cdot\zeta_w\omega\cos\psi e^{-kz}\cos\left(k\xi_G+kx\cos\psi\right) \\ \hat{v}_{Rw} = v_R - \beta_2\cdot\zeta_w\omega\sin\psi e^{-kz}\cos\left(k\xi_G+kx\cos\psi\right) \end{cases} \quad (11)$$

SYSTEM IDENTIFICATIONS FOR WAVE MODEL

To predict wave forces/effects, it is necessary to extract the wave forces/effects from total hydrodynamic forces. To achieve this purpose, first 6DOF CFD free running simulations in waves are executed. Second, CFD forced motion simulations in calm water are performed with imposing exactly the same motions as the free running simulation. Thus the wave forces/effects are estimated as the difference between the total force of the first and second simulations. Figure 6 shows the comparison between the extracted wave force using the CFD simulations and the computed ones without using tuning parameters during captive and free running in stern waves (H/λ=0.02, λ/L=1.0). The solid lines indicate the extracted wave forces and the dotted line shows the computed ones. There are some disagreement between the extracted wave forces and the computed ones. Especially during the zigzag maneuver, in range (3) in Fig.6, the gaps between extracted and computed ones are large. To cover these gaps, the CLS method is applied to predict the tuning parameters similar to the calm water maneuvering case (Araki et al, 2012a). Table4 shows the tuning parameters estimated by the above procedure. In Fig.7, by using those tuning parameters, the agreement between the extracted wave forces and computed ones are remarkably improved.

Table4 SI tuning result for SB wave model with Froude-Krylov, diffraction, maneuvering coefficients variation, and wave particle velocity.

Coef.	Orig.	SI-wave	**Coef.**	Orig.	SI-wave
a_1	1.0	0.758	c_1	1.0	0.832
a_2	0.0	16.33	c_2	0.0	0.510
a_3	0.0	0.855	c_3	0.0	0.195
a_4	0.0	0.132	ε_{c1}	0.0	0.0
ε_{a1}	0.0	0.0498	ε_{c2}	0.0	-0.99
ε_{a2}	0.0	0.391	ε_{c3}	0.0	1.03
ε_{a3}	0.0	3.21	d_1	1.0	9.81
ε_{a4}	0.0	0.0	d_2	0.0	1.01
b_1	1.0	3.68	d_3	0.0	0.213
b_2	0.0	2.18	ε_{d1}	0.0	1.68
b_3	0.0	0.496	ε_{d2}	0.0	0.982
ε_{b1}	0.0	0.0	ε_{d3}	0.0	-0.99
ε_{b2}	0.0	-0.552	β_1	1.0	0.643
ε_{b3}	0.0	0.810	β_2	1.0	0.425

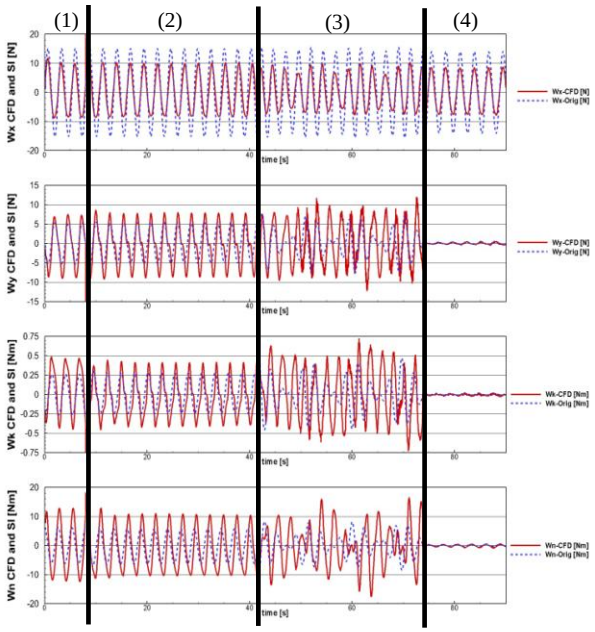

Fig.6 Wave force comparison between CFD and SB-Orig with Froude-Krylov and diffraction component with H/λ=0.02, λ/L=1.2; (1) captive running with χ=20deg, Fr=0.20; (2) course keeping free running with χ_c =20deg, nominal Fr=0.20 (3) 20/20 zigzag free running with nominal Fr=0.20; (4) free running in following waves with nominal Fr=0.20.

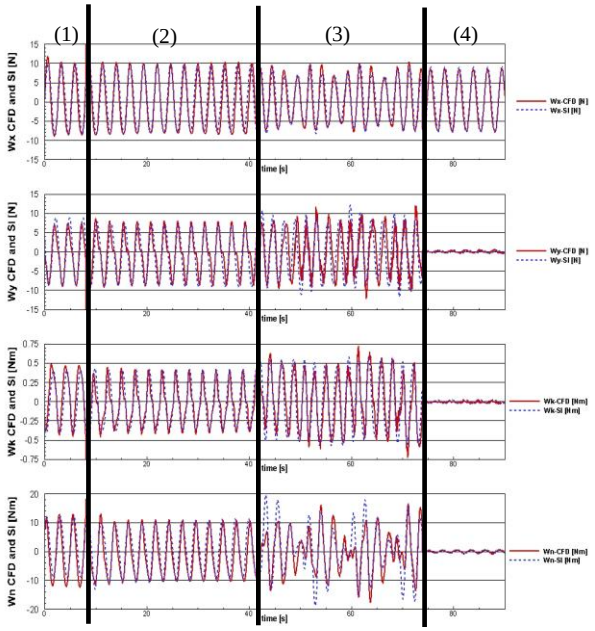

Fig.7 Wave force comparison between CFD and SB-SI with Froude-Krylov, diffraction, and maneuvering coefficients variation components in H/λ=0.02, λ/L=1.2; (1) captive running with χ=20deg, Fr=0.20; (2) course keeping free running with χ_c =20deg, nominal Fr=0.20 (3) 20/20 zigzag free running with nominal Fr=0.20; (4) free running in following waves with nominal Fr=0.20.

SB TIME DOMAIN SIMULATION USING SYSTEM IDENTIFICATION RESULTS

Using 4DOF SB model with the correction parameters shown in Table 4, estimated in last chapter, time domain SB simulations are executed and validated with EFD or/and CFD free running results.

(1) In Moderate Wave Condition

Straight running, course keeping and zigzag maneuver in moderate stern waves are simulated.

Figure 8 shows the straight running in following waves with nominal Fr=0.20, wave steepness 1/50 and wave length to ship length ratio 1.0. Here "SB-SIcalm" indicates SB simulation using maneuvering and rudder coefficients estimated by SI from CFD calm water maneuvering data (Araki et al., 2012a) with original wave model. "SB-SIwave" indicates SB simulations using same maneuvering and rudder coefficients with "SB-SI-calm" but with the modified wave model using tuning parameters identified from the CFD wave forces/effects data. Here, CFD shows remarkable agreement with EFD in surge velocity which indicates CFD has enough ability to predict ship motion in this wave condition. Moreover, it also shows using the CFD wave forces is apropriate for system identification. However "SB-SIcalm" slightly overestimates the surging amplitude while the "SB-SIwave" shows very close result with the CFD and EFD values.

Figure 9(1) and 10 show the comparison between CFD and "SB-SIcalm" χ_C=20deg course keeping in quartering waves with nominal Fr=0.20, wave steepness 1/50 and wave length to ship length ratio 1.0. Here the EFD and CFD rudder control start just after the model is released at a wave trough. Fig.9(1) shows good agreementfor the EFD and CFD course deviations due to wave force . However, EFD shows wobbly trajectory compared to CFD due to large oscillations for sway motions (see Fig. 10). Due to the sway motion error, the roll rate shows some difference

between EFD and CFD while the error is much smaller than that of sway motion. However, CFD successfully predicts the surge and yaw motions in quartering waves. Paying attention to CFD and SB results, "SB-SIcalm" shows small course deviation compared to that of CFD while the "SB-SIwave" shows close deviation with that of CFD. From the state variables comparisons (see Fig. 10), , it is clear that "SB-SIcalm" has some discrepancy on the wave forces compared to CFD and EFD. "SB-SIcalm" wave model overestimates the surge wave force and underestimates the sway, roll, and yaw wave forces. The "SB-SIwave" shows better agreement with CFD than "SB-SIcalm" for both state variables and the trajectory.

Figure 9(2) and 11 show the comparison between EFD, CFD and SB 20/20 zigzag in following and quartering waves with nominal Fr=0.20, wave steepness 1/50 and wave length to ship length ratio 1.0. The CFD results show good agreement with EFD for trajectory, surge, and yaw motions again. In sway motion, CFD seems underestimating the wave force compared to EFD which could explain the discrepancy of the roll motion. For the state variable time serises, the "SB-SIcalm" results show qualitative agreement with EFD maneuver but not quantitative. Moreover, the "SB-SIcalm" overestimates surge wave force and underestimates sway, and yaw wave forces. The "SB-SIwave" improves the prediction as it shows the oscillations on the state variables induced by the waves. Also, the speed loss is predicted well.

In moderate wave condition, the original SB simulations shows qualitative agreement with EFD. However the SB simulation using the tuning parameter estimated from CFD wave forces improve the accuracy of ship motion prediction especially for the ocillation amplitude due to wave. This could be the profit from the system identification.

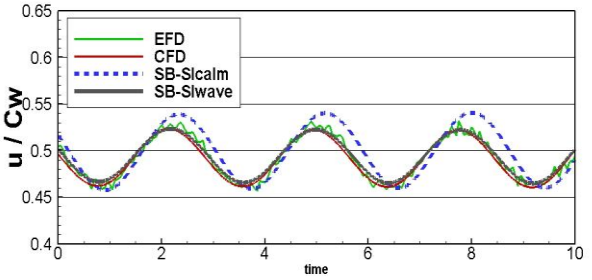

Fig.8 Comparisons of surge velocity between EFD, CFD, SB simulation with original wave model, and SB simulation with modified wave model using tuning parameters during straight free running in H/λ=0.02, λ/L=1.2 following wave with nominal Fr=0.20.

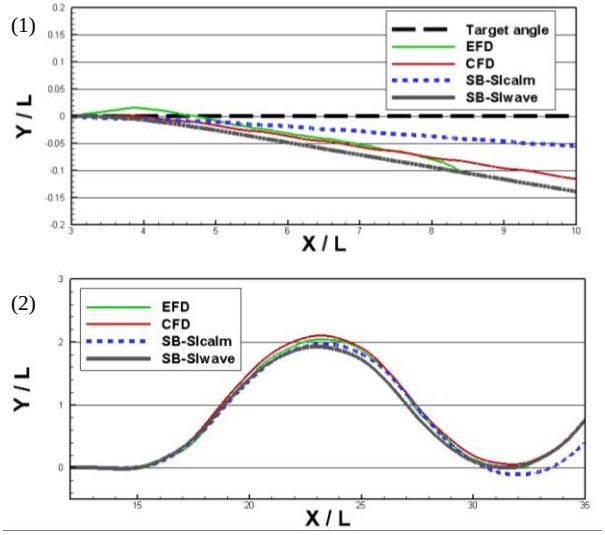

Fig.9 Trajectories in H/λ=0.02, λ/L=1.2; (1) course keeping free running with χ_c=20deg, nominal Fr=0.20; (2) 20/20 zigzag free running with nominal Fr=0.20.

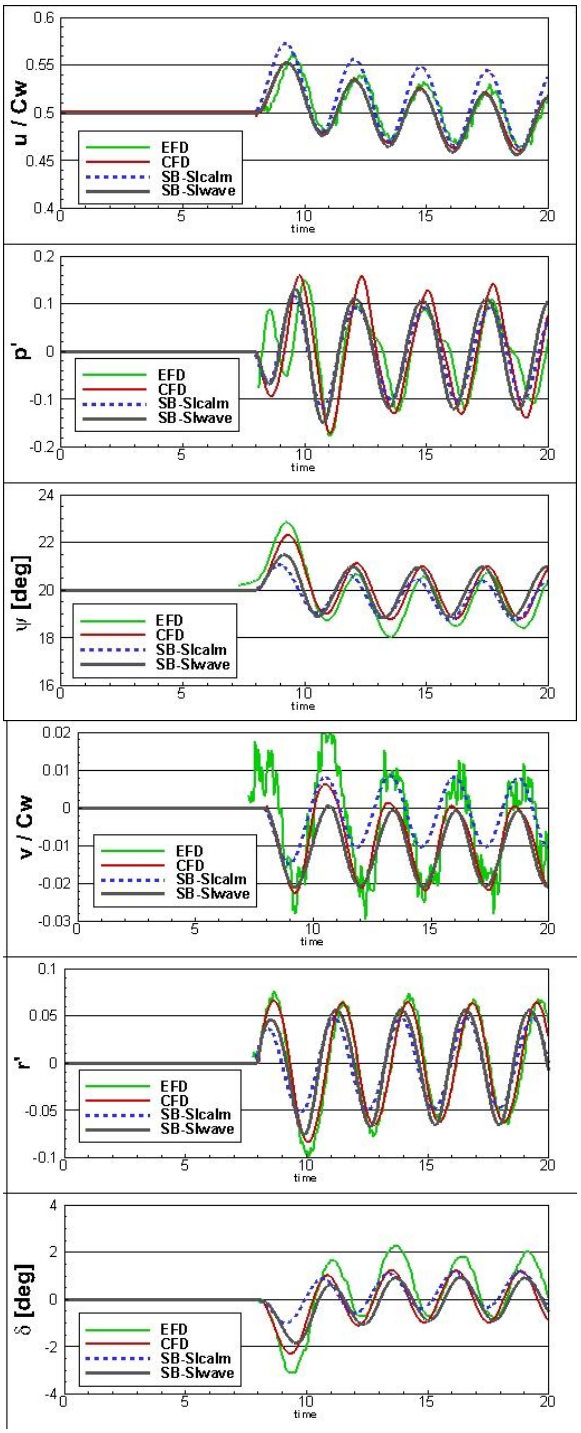

Fig.10 Time series during course keeping free running with χ_c=20deg, nominal Fr=0.20 in H/λ=0.02, λ/L=1.2.

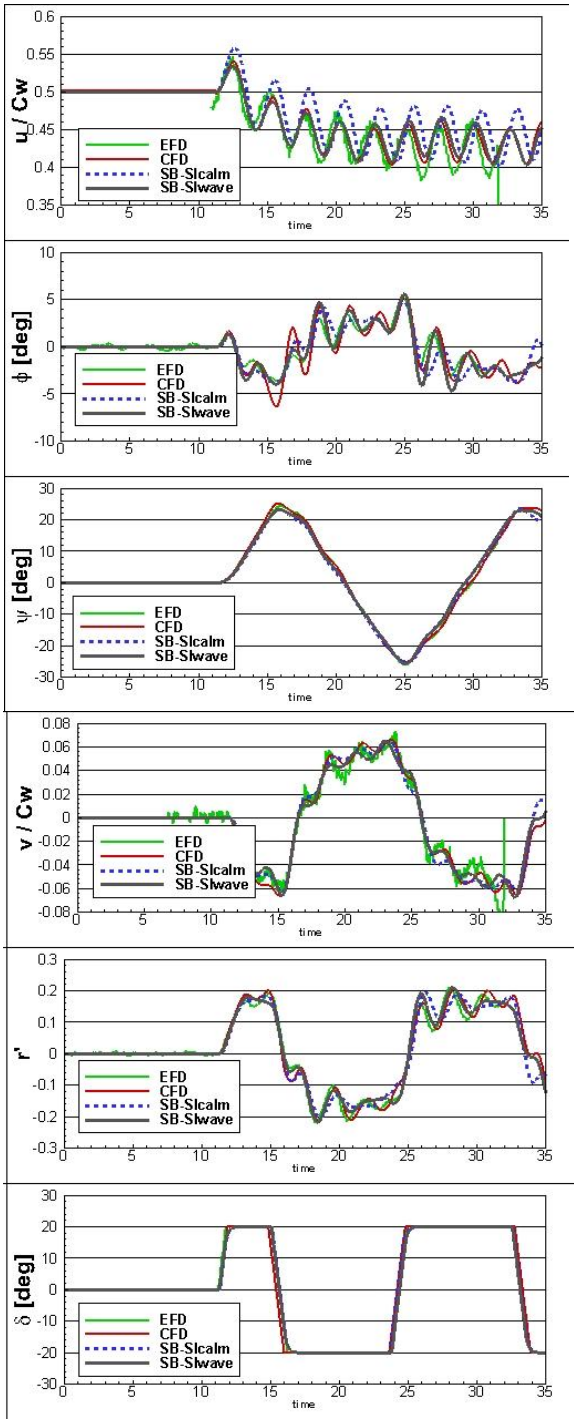

Fig.11 Time series during 20/20 zigzag free running with nominal Fr=0.20 in H/λ=0.02, λ/L=1.2.

(2) In Broaching Condition

To avoid maneuvering instability including broaching, it is important to specify dangerous operational conditions such as dangerous auto pilot course and ship speed. Using the SB model, the numerical simulation was executed for 4900 combinations of 70 auto pilot courses and 70 specified propeller revolutions represented as the nominal *Fr*, which is found in calm water with the specified propeller revolutions. The modes of ship motions are categorized into 6 groups: "Harmonic motion", "Stable surf-riding", "Capsizing without broaching", "Capsizing due to broaching", "Broaching without capsizing", and "Not identified" as these modes. The detail of the categorize definition is provided by Umeda et al. (2006). Herein the simulated "Harmonic motion" is colored in green, "Stable surf-riding" in blue, "Capsize without broaching" in black, "Broaching without capsizing" in orange, "Capsize due to broaching" in red, and "Not identified" is shown with white blank in the instability maps. The experimental "Harmonic motion-EFD" is shown with circle blanked marker, "Surf-riding-EFD" with diamond, and "Broaching" with triangle. The initial conditions for the SB simulation are computed based on sudden change concept (SCC) proposed by Umeda et al. (2002). Herein the course keeping maneuver starts when the ship situates at a wave trough during straight free running with nominal *Fr*=0.20 in pure following wave.

Figure 12 shows comparison between EFD free running results (Umeda et al., 2008) and SB simulation using identified maneuvering coefficients, listed in Table 3, and original wave model. Although the SB simulation results match with EFD results around small auto pilot course, there are large discrepancies in other area.

Figure 13 shows a comparison between EFD free running results and SB simulation using identified maneuvering coefficients listed in Table 3 and modified wave coefficients listed in Table4. The instability area, "Capsize" black area, suddenly increases showing large discrepancy with EFD.

In Fig.14, the SB wave model excluding variation of maneuvering coefficients components, tuned FK and diffraction coefficients values shown in Table5, is used for SB simulation. Even though these tuning parameters show some discrepancies for SI in Fig.13, this simplest model well predicts both surf-riding and broaching thresholds.

These results indicate the original wave model shows too stable maneuverability but the modified wave model including variation of maneuvering coefficients shows too unstable maneuverability. The modified wave model overestimates the variations of maneuvering coefficients in severe waves even though it shows reasonable results in moderate waves. Eqs. (5)-(8) indicate the variation will increase linearly with wave height. This assumption may cause this unnecessary instability. Son and Nomoto (1982) mentioned the variation of the maneuvering coefficients is induced by the variation of the form of the submerged profile due to wave. However the submerged profile does not change linearly with wave height. Therefore, the tuning parameters predicted in moderate wave cannot be applied to the severe wave cases. In this case, the model itself should be modified or the tuning parameters should be optimized in each target wave conditions. On the other hand, the result of Fig.14 indicates the tuning parameter in FK and diffraction forces predicted in moderate wave can be applied directly to severe wave cases.

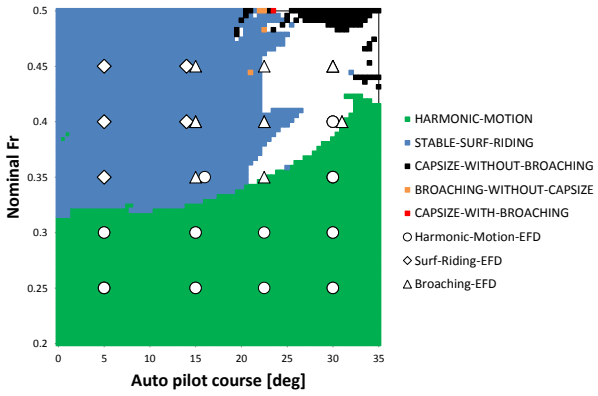

Fig.12 Ship motion comparison between free running experiments and SB using original wave model in H/λ=0.05, λ /L=1.25.

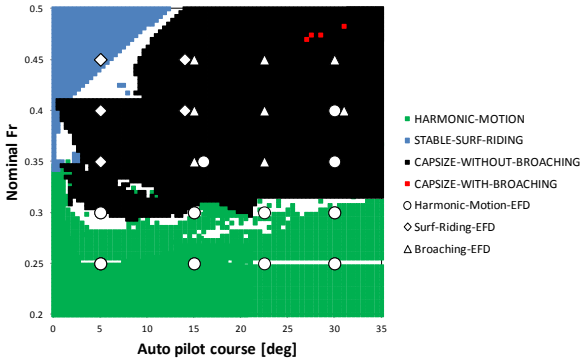

Fig.13 Ship motion comparison between free running experiments and SB using modified and tuned wave model in H/λ=0.05, λ /L=1.25.

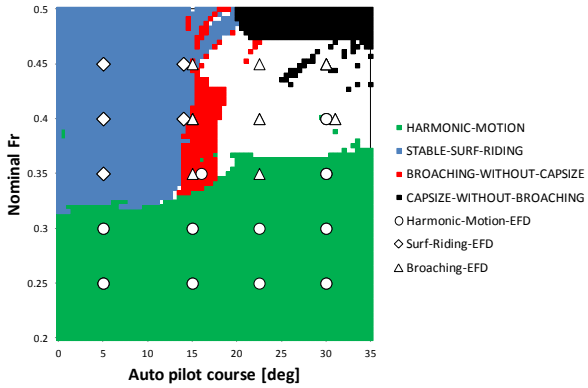

Fig.14 Ship motion comparison between free running experiments and SB using modified and tuned wave model excluding maneuvering coefficients variations components in H/λ=0.05, λ /L=1.25.

Table 5 SI tuning result for SB wave model with Froude-Krylov and diffraction components.

Coef.	Orig	SI	**Coef.**	Orig	SI
a_1	1.0	0.745	c_1	1.0	0.937
ε_{a1}	0.0	0.0613	ε_{c1}	0.0	0.0
b_1	1.0	3.72	d_1	1.0	8.81
ε_{b1}	0.0	0.0	ε_{d1}	0.0	1.68

CONCLUDING REMARKS

System identification method using CFD free running data is shown to be an efficient approach for estimating maneuvering, rudder, and wave correction coefficients in the SB model. Araki et al. (2012a) showed the reasonable maneuvering and rudder coefficients can be obtained from a few CFD free running data in calm water. The original SB model includes the Froude-Krylov and diffraction forces for the wave forces and includes wave particle velocity for the wave effect on the propeller and rudder. However the SB model using the original wave model still shows some errors predicting the ship motion in waves. Therefore, the SB wave model is improved by adding tuning parameters for FK, diffraction forces, and wave particle velocity. Moreover, effects of maneuvering coefficient variations due to waves are taken into account and these correction parameters are predicted by CLS using the extracted CFD wave forces/effects data. The extracted CFD wave forces/effects data are generated from the CFD free running data in waves and CFD forced motion data in calm water.

In moderate wave cases, the SB simulations using the new wave model and estimated wave correction coefficients show better agreement with CFD than the SB simulations using the original wave model. However, the model has some difficulties for, broaching prediction in severe wave conditions. This is due to the fact that the correction parameters are estimated for moderate wave while the broaching happens in more severe wave and higher speed conditions. The broaching predictions using SB method with different types of wave model and modifications showed that the maneuvering coefficients variation components have a crucial role to determine the ship motions mode and the linear assumptions respect to wave height seem to be inappropriate. Also, the simplest modified wave model, just tuning Froude-Krylov force and diffraction force, provides most reasonable prediction. In near future, new CFD simulations to be used for the SI, will be conducted and validated for different ship speeds and wave conditions, including more severe condition with higher ship speed and severe wave condition near to broaching conditions so that more appropriate parameters for broaching prediction could be estimated.

ACKNOWLEDGEMENTS

The research performed at IIHR was sponsored by the US Office of Naval Research, grants N00014-01-1-0073 and NICOP N00014-06-1-064 under

administration Dr. Ki-Han Kim. The CFD simulations were conducted utilizing DoD HPC. The authors are grateful to IIHR, NRIFE, Osaka University staffs and students for the experiments assistance. Finally, I would like to appreciate staffs of National Maritime Research Institute, Japan, for giving me an opportunity to present this paper.

REFERENCES

Araki, M., Umeda, N., Hashimoto, H., and Matsuda, A., 2010, Broaching Prediction Using an Improved System-Based Approach, Proceedings of 28th Symposium on Naval Hydrodynamics, 2010, pp. 56-68.

Araki, M., Sadat-Hosseini, H., Sanada, Y., Tanimoto, K., Umeda, N., and Stern, F., 2012a, Estimating Maneuvering Coefficients using System Identification Methods with Experimental, System-based, and CFD Free-running Trial Data, Ocean Engineering, Vol. 51, pp. 63-84.

Araki, M., Sadat-Hosseini H., Sanada, Y., Umeda, N. and Stern, F. 2012b, Study of System-based Mathematical Model Using System Identification Technique with Experimental, CFD, and System-Based Free Running Trials in Folllowing Waves, Proceedings of the 11th International Conference on Stability of Ships and Ocean Vehicles, Athens, pp. 171-185.

Bishop, R., Belknap, W., Turner, C., Simon, B., Kim, J., 2005, Parametric Investigation on the Influence of GM, Roll Damping, and Above-Water Form on the Roll Response of Model 5613, Report NSWCCD-50-TR-2005/027.

Carrica, P. M., Huang, J., Noack, R., Kaushik, D., Smith, B., and Stern, F., 2010, Large-scale DES computations of the forward speed diffraction and pitch and heave problems for a surface combatant, Computer &Fluids, Vol. 39, Issue 7, pp. 1095-1111.

Furukawa, T., Umeda, N., Matsuda, A., Terada, D., Hashimoto, H., Stern, F., Araki M., and Sadat-Hosseini, H., 2012, Effect of Hull Forms above Calm Water Plane on Extreme Ship Motions in Stern Quartering Waves, Proceedings of 28th Symposium on Naval Hydrodynamics, Gothenburg, Sweden, USB disk.

Hashimoto, H., Umeda, N., and Matsuda, A., 2011, Broaching prediction of a wave-piercing tumblehome vessel with twin screws and twin rudders, Journal of Marine Scienece and Technology, Vol. 16, pp. 448-461.

IMO, 2012, Report to the Maritime Safety Committee, SLF 54/17.

Ogawa, A., and Kasai, H., 1978, On the Mathematical Model of Maneuvering Motion of Ship, International Shipbuilding Progress, Vol. 25, No. 292, pp. 306-319.

Ogawa, A., Hasegawa, K., and Yoshimura, Y., 1980, MMG report V, Bulletin of Society of Naval Architects of Japan, No. 616, pp. 565–576.

Sadat-Hosseini, H., Carrica, M. P., Stern, F., Umeda, N., Hashimoto, H., Yamamura, S., and Mastuda, A., 2011, CFD, system-based and EFD study of ship dynamic instability events: surf-riding, periodic motion, and broaching, Ocean Engineering, Vol. 38, Issue 1, pp. 88-110.

Sanada, Y., Tanimoto, K., Takagi, K., Sano, M., Yeo, D. J., Toda, Y., and Stern, F., 2012, Trajectories of Local Flow Field Measurement around ONR Tumblehome in Maneuvering Motion, Proceedings of The 29th Symposium on Naval Hydrodynamics, Gothenburg, Sweden, USB disk.

Son, K. H., and Nomoto, K., 1982, Combined behavior of maneuvering and roll motion in following wave, Journal of the Society of Naval Architects of Japan, Vol. 152, pp. 207-218.

Umeda, N., 1999, Nonlinear Dynamic on Ship Capsizing due to Broaching in Following and

Quartering Seas, Journal of Marine Science and Technology, Vol. 4, pp. 16-27.

Umeda, N., and Hashimoto, H., 2002, Qualitative Aspect of Nonlinear Ship Motion in Following and Quartering Seas with High Forward Velocity, Journal of Marin Science and Technolocy, Vol. 6, pp. 111-121.

Umeda, N., Maki, A. and Hashimoto, H., 2006, Maneuvering and Control of a High-Speed Slender Vessel with Twin Screws and Twin Rudders in Following and Quartering Seas, Journal of the Japan Society of Naval Architects and Ocean Engineers, Vol. 4, pp. 155-164.

Umeda, N., Yamamura, S., Matsuda, A., Maki, A., and Hashimoto, H., 2008, Model Experiments on Extreme Motion of Wave-Piercing Tumblehome Vessel in Following and Quartering Waves, Journal of Japan Society of Naval Architects and Ocean Engineers, Vol. 8, pp. 123-129.